Simulation of random field samples directly from sparse measurements using Bayesian compressive sampling and Karhunen‐Loève expansion

Yue Hu
Graduate Student, City University of Hong Kong, Hong Kong

Yu Wang
Associate Professor, City University of Hong Kong, Hong Kong

Tengyuan Zhao
Research Associate, City University of Hong Kong, Hong Kong

ABSTRACT: Geotechnical materials (e.g., soils and rocks) are natural materials, and they are affected by many spatially varying factors during the geological process, such as properties of their parent materials, weathering and erosion processes, transportation agents, and sedimentation conditions. Geotechnical data therefore exhibit spatial variability, and to some extent, are unique in every site. In recent years, random field has been increasingly used to model spatial variability of geotechnical data. In conventional frequentist approach, measurement data at a specific site are used to estimate random field parameters, such as mean and standard deviation, as well as parameters (e.g., correlation length) of a pre-determined parametric form of correlation function (e.g., an exponential correlation function). Estimation of these random field parameters, particularly the correlation length, and selection of the suitable parametric form of correlation function generally require extensive measurements from a specific site, which are generally not available in geotechnical engineering practice. This paper presents a random field generator that is able to simulate random field samples directly from sparse measurements, bypassing the difficulty in the estimation of correlation function and its parameters. The proposed generator is based on Bayesian compressive sensing/sampling and Karhunen‐Loève expansion. The proposed method is illustrated and validated using simulated geotechnical data. It is also compared with the conventional random field models. The results show that the proposed generator can rationally simulate the geotechnical spatial variability at a specific site from sparse measurements.

Keywords: site characterization, Bayesian method, compressed sensing, random field

Geo-materials (e.g., soils and rocks) are natural materials, and they are affected by many spatially varying factors during their complex geological formation process, such as the textures of their parent materials, weathering and erosion processes, transportation agents, and sedimentation conditions (e.g., Baecher and Christian 2003). These environmental factors are spatially varying and make the characteristics of soils and rocks different at different locations. Geotechnical properties therefore exhibit spatial variability, and to some extent, are unique in every site (e.g., Webster 2000) as a deterministic outcome of the previous geological processes. This means that the spatial variability of geotechnical properties is site-specific. In other words, for a specific site, geotechnical properties at different locations may have different but deterministic values. Although the site-specific spatial variability is not stochastic but deterministic, the inherent spatial variability of geotechnical properties has often been modeled using random field theory for mathematical convenience (e.g., Stuedlein et al. 2012).

The conventional random field models generally use a series of auto-correlated random variables to simulate the spatial variability of geotechnical properties when measurements from site are sparse and limited. It can provide a statistical inference at unmeasured locations in a site and facilitate associated probabilistic analysis. The key of the random field models is to properly determine the random field parameters (e.g., mean, standard deviation as well as correlation structure of spatially varying geotechnical properties) before random field simulation. To objectively determine those parameters, measurement data at a specific site are often adopted. It should be note that, however, estimation of these random field parameters, particularly the correlation length generally requires extensive data from the specific site, which are usually not available in geotechnical practice (e.g., Wang and Zhao 2017). Because the underlying correlation function form is often unknown for a specific site, it is also challenging to select the most suitable parametric form of the correlation function when only limited measurements are available. In addition, when the amount of site measurement data is sufficiently large, e.g., geotechnical properties are measured at all locations in a specific site and the spatial variability becomes deteriministic, the random field models do not converge to the measurement data but still produce random pattern using the estimated random field parameters.

This paper presents a new random field generator that can address the above problems. The random field generator is based on Bayesian compressive sensing/sampling (BCS) and Karhunen‑Loève expansion (KL). The BCS-KL generates random field samples (RFS) of spatially varying geotechnical properties directly from sparse measurements and bypasses the challenge in estimating the random field parameters, especially the correlation length (Wang et al. 2018). Moreover, RFS generated by BCS-KL is convergent. When geotechnical data are available at all locations, the spatial variability is unique and deterministic. In this case, the RFS generated by BCS-KL also converge to the measurement data with negligible uncertainty.

In this study, the BCS method and KL expansion are first introduced. Then the proposed method is illustrated using a simulated example with comparison to conventional random field models.

1. BAYESIAN COMPRESSIVE SAMPLING AND KARHUNEN‑LOÈVE EXPANSION

1.1. Brief review of Bayesian compressive sampling

Bayesian compressive sampling/sensing (BCS) is a probabilistic method for reconstructing a signal from partial measurements on that signal (e.g., Ji et al. 2008; Wang and Zhao 2017). A signal is defined as variation of a spatiotemporal quantity. It is denoted as a real-valued vector $\boldsymbol{f}$ with length N. Partial measurements on $\boldsymbol{f}$ is denoted as an M-length column vector $\boldsymbol{y}$ (M<<N). In the context of BCS, $\boldsymbol{f}$ can be considered as a weighted summation of N orthonormal basis functions (e.g., wavelet functions), expressed as $\boldsymbol{f} = \mathbf{B}\boldsymbol{\omega}$ (e.g., Candès and Wakin 2008; Wang and Zhao 2016). $\mathbf{B}$ is an N × N matrix, with columns being the prescribed basis functions in different frequencies. $\boldsymbol{\omega}$ is an N-length column vector, representing the weights corresponding to $\mathbf{B}$. Note that, given an appropriate basis function (e.g., wavelet function) for $\mathbf{B}$, most elements of $\boldsymbol{\omega}$ are very small or virtually zero except of several non-trivial ones with significant magnitudes (e.g., Candès and Wakin 2008). Therefore, it is possible to reconstruct the signal $\boldsymbol{f}$ from $\boldsymbol{y}$, if the non-trivial coefficients of $\boldsymbol{\omega}$ are obtained from $\boldsymbol{y}$ using $\boldsymbol{y} = \boldsymbol{\Psi f} = \boldsymbol{\Psi B\omega} = \mathbf{A}\boldsymbol{\omega}$, where $\mathbf{A} = \boldsymbol{\Psi B}$ and $\boldsymbol{\Psi}$ is measurement matrix that represents the locations of components of $\boldsymbol{y}$ in $\boldsymbol{f}$. Herein, $\boldsymbol{\omega}_s$ is defined as approximation coefficients vector of $\boldsymbol{\omega}$ estimated from $\boldsymbol{y}$, with all components of $\boldsymbol{\omega}_s$ equal to zero except the S non-trivial components. When the limited measurement data $\boldsymbol{y}$ is used to estimate $\boldsymbol{\omega}_s$, the vector $\boldsymbol{\omega}_s$ might be inaccurate and contains significant statistical uncertainty (e.g.,

Wang and Zhao 2017). In such a case, $\boldsymbol{\omega}_s$ may be considered as a random vector, whose probability distribution can be derived under a Bayesian framework. It has been shown that $\boldsymbol{\omega}_s$ follows a multivariate Students' t distribution with degree of freedom $2c_n$, with a mean of $\boldsymbol{\mu}_{\omega_s}$ and covariance matrix of $\mathbf{COV}_{\omega_s}$, which are expressed as (e.g., Wang and Zhao 2017):

$$\boldsymbol{\mu}_{\omega_s} = \mathbf{H}\mathbf{A}^{\mathrm{T}}\boldsymbol{y} = \left(\mathbf{A}^{\mathrm{T}}\mathbf{A}+\mathbf{D}\right)^{-1}\mathbf{A}^{\mathrm{T}}\boldsymbol{y}$$
$$\mathbf{COV}_{\omega_s} = \frac{d_n\mathbf{H}}{c_n-1} = \frac{d_n\left(\mathbf{A}^{\mathrm{T}}\mathbf{A}+\mathbf{D}\right)^{-1}}{c_n-1} \quad (1)$$

in which $\mathbf{H} = (\mathbf{A}^{\mathrm{T}}\mathbf{A}+\mathbf{D})^{-1}$; $c_n = \mathrm{M}/2+c_0$; $d_n = d_0+(\boldsymbol{y}^{\mathrm{T}}\boldsymbol{y}-\boldsymbol{\mu}_{\omega_s}{}^{\mathrm{T}}\mathbf{H}^{-1}\boldsymbol{\mu}_{\omega_s})/2$; c_0 and d_0 are small non-negative constants (e.g., $c_0 = d_0 = 10^{-4}$); $\mathbf{D}$ = a diagonal matrix with diagonal elements being $\mathrm{D}_{i,i} = \alpha_i$ (i = 1, 2, …, N); α_i (i = 1, 2, …, N) are unknown non-negative hyper-parameters, which can be determined by iterative algorithm when the likelihood of $\boldsymbol{y}$ reaches its maximum (e.g., Tipping 2001; Ji et al. 2008; Wang and Zhao 2017). Although the whole matrices $\mathbf{A}$ and $\mathbf{D}$ are involved in Eq. (1), only the first S columns of $\mathbf{A}$ and the first S diagonal elements α_i (i.e., α_i, i = 1, 2, …, S, and S<<N) of matrix $\mathbf{D}$ are needed in applications. This is because the first S columns of $\mathbf{A}$ and α_i (i = 1, 2, …, S) of matrix $\mathbf{D}$ correspond to the S non-trivial coefficients (i.e., the first S elements of $\boldsymbol{\omega}$) when discrete wavelet transform is used to construct $\mathbf{B}$. Therefore, only the first S elements of $\boldsymbol{\mu}_{\omega_s}$ and the first S rows by the first S columns of $\mathbf{COV}_{\omega_s}$ need to be estimated, while the remaining elements are set to zero. Based on the definition of mean and covariance matrix, the mean $\boldsymbol{\mu}_{\hat{f}}$ and covariance $\mathbf{COV}_{\hat{f}}$ of the reconstructed signal $\hat{\boldsymbol{f}}$ are derived as (e.g., Wang and Zhao 2017):

$$\boldsymbol{\mu}_{\hat{f}} = \mathrm{E}(\hat{\boldsymbol{f}}) = \mathrm{E}(\mathbf{B}\boldsymbol{\omega}_s) = \mathbf{B}\,\mathrm{E}(\boldsymbol{\omega}_s) = \mathbf{B}\boldsymbol{\mu}_{\omega_s}$$
$$\mathbf{COV}_{\hat{f}} = \mathrm{E}[(\hat{\boldsymbol{f}}-\boldsymbol{\mu}_{\hat{f}})(\hat{\boldsymbol{f}}-\boldsymbol{\mu}_{\hat{f}})^{\mathrm{T}}] = \mathbf{B}\mathbf{COV}_{\omega_s}\mathbf{B}^{\mathrm{T}} \quad (2)$$

Given multivariate statistics of the estimated signal, it is possible to generate RFS of $\hat{\boldsymbol{f}}$ via Karhunen–Loève expansion.

1.2. Karhunen–Loève expansion

Karhunen – Loève (KL) expansion is a representation of stochastic process via linear combination of a series of deterministic and orthogonal eigenfunctions. It has been widely used to simulate various random processes in engineering. In essence, KL expansion decomposes the covariance function of the stochastic process of interest into a series of eigenfunctions. In discrete case, it is equivalent to eigenvalue decomposition of a covariance matrix of a discrete random process. Using the mean value vector and associated covariance matrix in Eq. (2), BCS-based RFS of $\hat{\boldsymbol{f}}$ can be generated under KL expansion framework (e.g., Phoon et al. 2002; Au and Wang 2014; Wang et al. 2018):

$$\hat{\boldsymbol{f}} = \boldsymbol{\mu}_{\hat{f}} + \mathbf{V}\sqrt{\mathbf{COV}_{\hat{f},d}}\,\boldsymbol{Z} \quad (3)$$

where $\mathbf{V}$ is the eigenvector matrix of $\mathbf{COV}_{\hat{f}}$; $\mathbf{COV}_{\hat{f},d}$ is a diagonal matrix that records the eigenvalues of $\mathbf{COV}_{\hat{f}}$; $\boldsymbol{Z}$ is a set of uncorrelated standard random variables, with zero-mean and unit-variance. For convenience, $\boldsymbol{Z}$ is often taken as a random vector with uncorrelated standard Gaussian numbers. According to Eq. (3), RFS of $\hat{\boldsymbol{f}}$ can be obtained readily by realization of uncorrelated random vector $\boldsymbol{Z}$.

A schematic of the proposed BCS-KL method is shown in the Figure 1. A soil mechanical property (e.g., the X) along depth is adopted as an illustration. When limited measurements versus depth are taken (i.e., the open circles) at a specific site, BCS provides the best estimate of the property X (e.g., the grey scale column) along depth including those unsampled locations, and a covariance matrix (e.g., the grey scale map). Thereafter, RFS (e.g., three grey lines) can be readily generated through KL expansion using $\boldsymbol{\mu}_{\hat{f}}$ and $\mathbf{COV}_{\hat{f}}$. It is seen that

the multivariate statistics of the spatial variability is estimated directly from sparse measurements without using a parametric form of correlation functions. It bypasses the difficulty of selecting appropriate parametric form of correlation function. The RFS generated via BCS-KL reflect prediction of the spatial variability from the sparse measurements objectively.

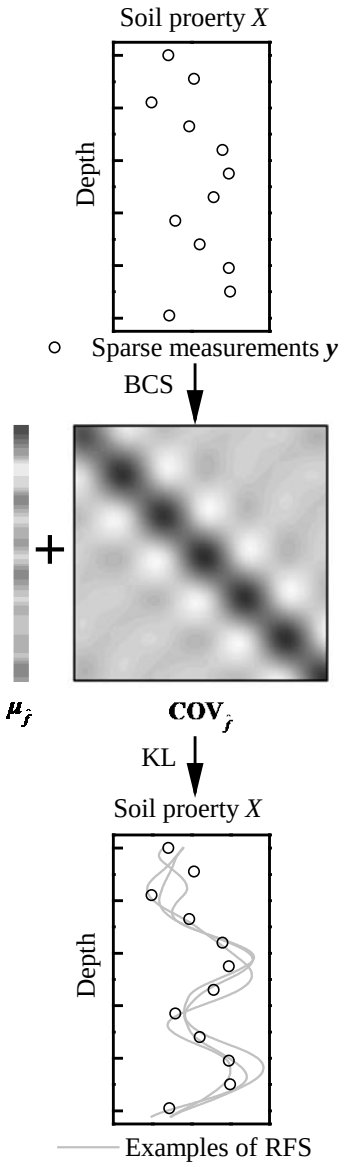

Figure 1: Schematic of the proposed BCS-KL method

In the next section, the proposed BCS-KL method is illustrated using a simulated example. The performance of conventional random field is also compared.

2. NUMERICAL EXAMPLE

In this section, a set of simulated data is adopted to illustrate the performances of the BCS-KL and conventional random field. In this example, a soil property *X* profile within a 20.44m-thick soil layer in a specific site is simulated with a resolution of 0.04m, as shown in Figure 2 by a black solid line. This profile has 512 data points, and it represents spatial variability of soil property *X* at this specific site.

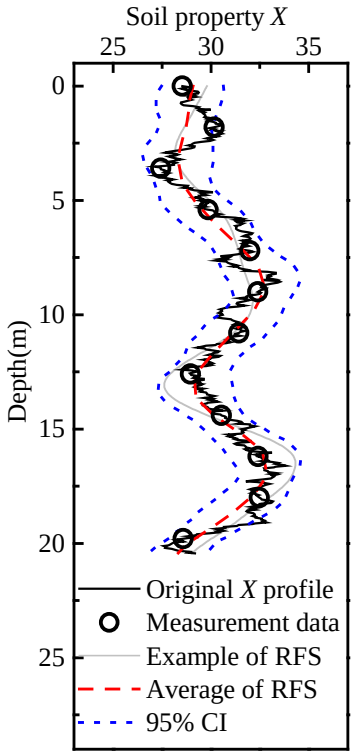

Figure 2: Results of BCS-KL generator

Note that the original *X* profile (i.e., the black solid line in Figure 2) is only used for illustration and validation, and it is unknown in real geotechnical engineering practice. In this example, the *X* profile is simulated from a stationary Gaussian random field with a mean of 30 and a standard deviation (SD) of 2. In addition, a cosine exponential auto-correlation function (CSX) is adopted in this case, expressed as:

$$\rho(\tau) = \exp(-\frac{\tau}{\lambda})\cos(-\frac{\tau}{\lambda}) \qquad (4)$$

in which the $\rho(\tau)$ is the auto-correlation function at lag distance "τ"; λ is the correlation length and

it is taken as 4m for generation of the *X* profile. To investigate the performances of the BCS-KL generator, as well as the conventional random field models, limited points (e.g., M=12 points shown in Figure 2) are sampled as measurements or input to generate RFS in this site. The results are demonstrated in the following subsections.

2.1. Results of BCS-KL generator

Following the procedure illustrated in Figure 1, RFS of *X* can be generated using KL expansion based on the BCS results from measurement data. An example of RFS of *X* is shown in Figure 2 by a gray line. Although only 12 measurement points versus their locations are used as input, the RFS properly reflects the general spatial variation of the underlying site-specific data. In this subsection, 1000 sets of RFS are generated using the proposed BCS-KL method. Pointwise statistics (e.g., mean and SD) at each depth are calculated and shown in the Figure 2. The dashed line indicates the averaged profile of 1000 RFS. The two dotted lines indicates the 95% confidence interval (CI) of 1000 RFS, which correspond to the 2.5th and 97.5th percentiles of 1000 RFS values at each depth. It can be noted that the averaged profile follows a trend consistent with the measurement data, and almost all local variations of the black solid line fall within the 95% CI. This implies that the spatial variation of *X* is rationally characterized by RFS from limited measurements.

The spatial auto-correlation embedded in the *X* profiles can be quantified by the auto-covariance function (AF), which is calculated using Eq. (5):

$$C(\delta) = \frac{1}{\mathrm{N}-\delta}\sum_{i=1}^{\mathrm{N}-\delta}[(\hat{f}_i - \mu)(\hat{f}_{i+\delta} - \mu)] \qquad (5)$$

where $C(\delta)$ represents the estimator of AF at δ; δ is the lag distance (in terms of integer in this example) between the i-th and the $(i + \delta)$-th element, i.e., $\hat{f}_i$ and $\hat{f}_{i+\delta}$; and μ represents the mean of $\hat{\boldsymbol{f}}$. Using Eq. (5), the AF of the underlying *X* profile is calculated and shown in Figure 3 by a solid line. Note that the black solid line reflects the auto-correlation of the original *X* profile. The AF for each of the simulated 1000 RFS can also be calculated using Eq. (5). This leads to 1000 AF. Then the average and 95% CI of 1000 AF can be obtained at each lag distance, as shown in Figure 3 by a dashed line and a pair of dotted lines, respectively. AF of the RFS example in Figure 2 is also plotted as grey line in Figure 3.

Figure 3 shows that both the gray and dashed lines decreases as the lag distance increases, following a pattern similar to the black solid line. Moreover, noted that all local variations of the solid lines fall within the 95% CI depicted by the two dotted lines. These agreements indicate that the spatial auto-correlation embedded in the original *X* profile is properly captured by 1000 RFS generated using the proposed BCS-KL generator. Also, the uncertainty of the estimated AF is properly quantified. Note that the above RFS generation does not involve estimation of a parametric form of correlation function. The discussion on the conventional random field is provided in the following subsection.

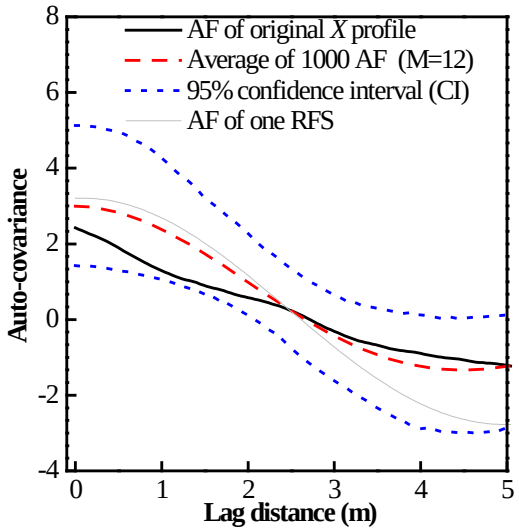

Figure 3: AF of original X profile and RFS generated by BCS-KL

2.2. Results of random field with assumed correlation function form

The frequently used random field model requires the random field parameters (e.g., mean, variance,

correlation length) to be determined before RFS generation. The determination of auto-correlation function is a tricky issue because both the function form and correlation parameters are unknown for a given site, not to mention that the real data might contain trend and are non-stationary (e.g., Wang et al. 2019). Usually, experimental auto-correlation is estimated based on measurements. For example, using the measurement data (i.e., open circles) in Figure 2, the experimental AF at several lag distances are obtained from Eq. (5) and shown in Figure 4 by open circles. Then, a pre-specified correlation function form, e.g., frequently used single exponential correlation structure (SNX), is used to best fit experimental AF. The SNX is expressed as:

$$\rho(\tau) = \sigma^2 \exp(-\frac{2\tau}{\lambda}) \quad (6)$$

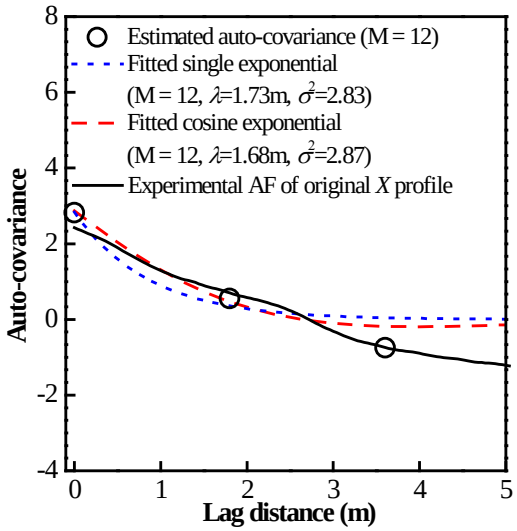

Figure 4: AF estimation from measurements in conventional random field models

The parameters of the SNX can be obtained from the best fitting. Figure 4 shows the fitted SNX by a blue dotted line, together with summary of the estimated parameters, i.e., 1.73 for the correlation length and 2.83 for variance in this example. After that, covariance structure can be constructed based on those parameters. Subsequently, RFS can be generated based on KL expansion or Cholesky decomposition (e.g., Au and Wang 2014) to characterize the spatial variability of X in the specific site. To be consistent with the previous subsection and make fair comparison, 1000 RFS are simulated, using which the average of RFS and 95% CI at each depth are calculated and shown in Figure 5a by a dashed line and two dotted lines, respectively.

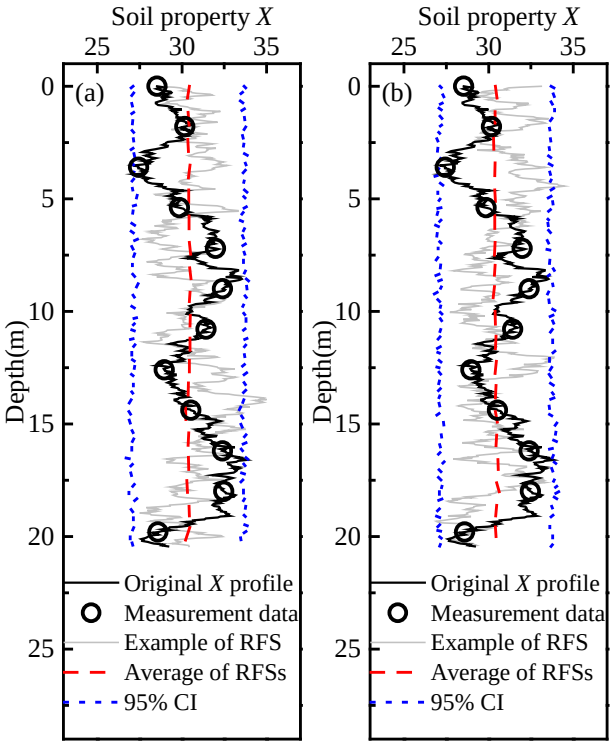

Figure 5: Results of conventional random field modeling: (a) single exponential AF; (b) cosine exponential AF

Figure 5a shows that the dashed line (i.e., the average of RFS) is almost a constant, which is obvious different with the spatial variation of the original X profile in this site (i.e., the black solid line). The discrepancy indicates that the RFS obtained from conventional random field modeling might not be representative of the spatial variability of X in this site, even when the parameters used in the simulation are estimated from the site-specific measurements (e.g., the open circles in Figure 2 and 5a).

The discrepancy observed above might be partly explained by the improper correlation function form (i.e., SNX) adopted in the

simulation. For further exploration, the correct correlation function form (i.e., CSX) for the original *X* profile is assumed to be known, and the parameter estimation and RFS simulation procedure described above for SNX are repeated. In this case, the correlation length and variances are estimated as 1.68 and 2.87, respectively. The estimated parameters and best-fitted CSX function are also shown in Figure 4. Then, 1000 RFS are generated using the CSX correlation function and the above parameters. One RFS example and statistics of those 1000 RFS are shown in the Figure 5b. Note that the average of RFS (i.e., the dashed line Figure 5b) is also a constant, similar to that in Figure 5a. In other words, even if the correct correlation function form is known, the RFS simulated under the conventional random field model still cannot properly reflect the site-specific spatial variation of *X*.

3. EFFECT OF NUMBER OF MEASUREMENT POINTS

To further explore the effect of number of measurement points M on the performances of the BCS-KL generator and conventional random field model, three more measurement scenarios, i.e., M = 25, M = 64, M = 512 are investigated.

3.1. Convergence behavior of BCS-KL

This subsection provides the results of BCS-KL RFS simulation under three more different M scenarios, i.e., M = 25, 64 and 512. For each scenario, M measurements with an equal interval are extracted from the black solid line in Figure 2&5 as input to BCS-KL to characterize the spatial variability of *X*. Following the same procedures, 1000 RFS of *X* are generated for each M scenario. Figure 6a to 6d summarize the results for M = 12, M = 25, M = 64, M = 512, respectively.

Figure 6 shows that as M increases, the RFS generated reflect an increasing amount of site-specific information. The average of 1000 sets of RFS (i.e., red dash lines) becomes increasingly similar to the original *X* profile (i.e., the black solid line). In addition, the 95% CI gradually reduces and approaches to zero effectively. When M=512, the generated RFS converge to the original *X* profile with negligible uncertainty.

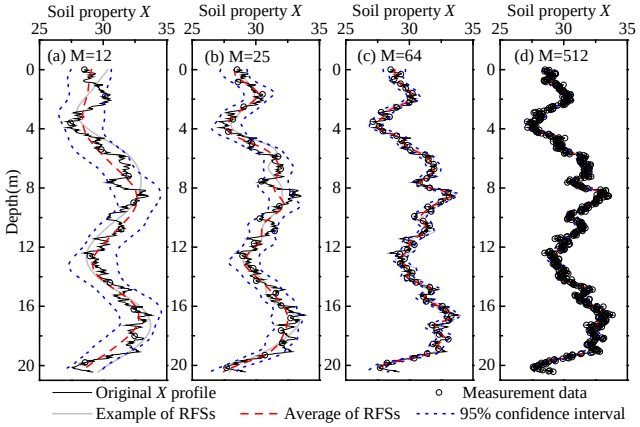

Figure 6: Effect of number of measurement points on the BCS-KL generator

3.2. Non-convergence behavior of conventional random field

The effect of number of measurement points M is also explored for the conventional random field models. The same measurement scenarios in the previous subsection are applied, with the assumption that the correct correlation structure, i.e., CSX correlation model, is known already. Following the same procedure as stated in the previous section, 1000 RFS are simulated for each M scenario using conventional random field model. The results are plotted in Figure 7a to 7d. Figure 7 shows that as the number of measurement data increases, the RFS simulated exhibit similar auto-correlation. In other words, the RFS obtained from conventional random field model does not seem to be affected by the measurement data quantity obtained within this specific site. The averaged profile (i.e., the dashed line) remains more or less constant, despite of the increase of measurement points number. When data at all locations are available, the conventional random field models still produce stochastic RFS rather than deterministic spatial variability. This result indicates that the conventional random field models cannot converge to the underlying spatial variability of geotechnical data even if measurements are sufficient.

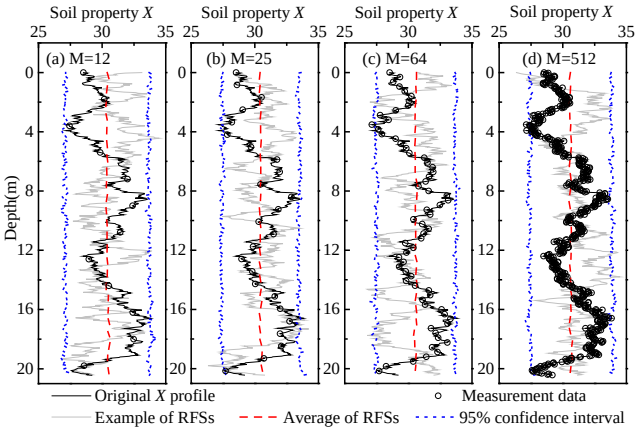

Figure 7: Effect of number of measurement points on conventional random field model

4. CONCLUSIONS

This study presents a new random field generator for simulating the spatial variability of geotechnical properties in a specific site. The proposed method is based on Bayesian compressive sampling (BCS) and Karhunen–Loève (KL) expansion, and abbreviated as BCS-KL generator. The proposed generator does not require estimation of parametric form of correlation function which is prerequisite in the conventional random field models. The BCS method and KL expansion are introduced first. Then the implementation of the method is demonstrated concisely through a schematic figure. A numerical example is presented to illustrate the effectiveness of the proposed method. Performance of conventional random field models is also compared in the study. The results show that the proposed method can generate RFS that objectively reflect the spatial variability of geotechnical properties. Moreover, as the number of measurements points increases, the RFS generated by BCS-KL converge the underlying true variability gradually.

5. ACKNOWLEDGEMENTS

The work described in this paper was supported by grants from the Research Grants Council of the Hong Kong Special Administrative Region, China (Project No. 9042331 (CityU 11225216) and Project No. 9042516 (CityU 11213117)). The financial support is gratefully acknowledged.

6. REFERENCES

Au, S.-K., and Wang, Y. (2014). Engineering risk assessment with subset simulation. John Wiley & Sons, Singapore (pp. 78-83).

Baecher, G.B., and Christian, J.T. (2003). Reliability and statistics in geotechnical engineering. John Wiley & Sons, Hoboken, New Jersey (pp. 228-239).

Candès, E.J., and Wakin, M.B. (2008). "An introduction to compressive sampling." IEEE Signal Proc. Mag., 25(2), 21-30.

Ji, S., Xue, Y., and Carin, L. (2008). "Bayesian compressive sensing." IEEE Trans. Signal Process., 56(6), 2346-2356.

Phoon, K.K., Huang, S.P., and Quek, S.T. (2002). "Simulation of second-order processes using Karhunen–Loeve expansion." Comput. Struct., 80(12), 1049-1060.

Stuedlein, A.W., Kramer, S.L., Arduino, P., and Holtz, R.D. (2012). "Geotechnical characterization and random field modeling of desiccated clay." J. Geotech. Geoenviron. Eng., 138(11), 1301-1313.

Tipping, M.E. (2001). "Sparse bayesian learning and the relevance vector machine." J. Mach. Learn. Res., 1, 211-244.

Wang, Y. and Zhao, T. (2016). "Interpretation of soil property profile from limited measurement data: a compressive sampling perspective." Can. Geotech. J., 53(9), 1547-1559.

Wang, Y., and Zhao, T. (2017). "Statistical interpretation of soil property profiles from sparse data using Bayesian compressive sampling." Géotechnique, 67(6), 523-536.

Wang, Y., Zhao, T., and Phoon, K.K. (2018). "Direct simulation of random field samples from sparsely measured geotechnical data with consideration of uncertainty in interpretation." Can. Geotech. J., 55(6), 862-880.

Wang, Y., Zhao, T., Hu, Y., and Phoon, K. K. (2019). "Simulation of random fields with trend from sparse measurements without de-trending." J. Eng. Mech., ASCE, 145(2), 04018130.

Webster, R., and Oliver, M.A. (2007). Geostatistics for environmental scientists. 2nd edition. John Wiley & Sons, Hoboken, New York (pp. 50-53).